

Journal of Materials Chemistry C

Accepted Manuscript



This is an *Accepted Manuscript*, which has been through the Royal Society of Chemistry peer review process and has been accepted for publication.

Accepted Manuscripts are published online shortly after acceptance, before technical editing, formatting and proof reading. Using this free service, authors can make their results available to the community, in citable form, before we publish the edited article. We will replace this *Accepted Manuscript* with the edited and formatted *Advance Article* as soon as it is available.

You can find more information about *Accepted Manuscripts* in the [Information for Authors](#).

Please note that technical editing may introduce minor changes to the text and/or graphics, which may alter content. The journal's standard [Terms & Conditions](#) and the [Ethical guidelines](#) still apply. In no event shall the Royal Society of Chemistry be held responsible for any errors or omissions in this *Accepted Manuscript* or any consequences arising from the use of any information it contains.

David O. Scanlon^{*, a, b}, John Buckeridge,^a C. Richard A. Catlow,^a and Graeme W. Watson^c

Received Xth XXXXXXXXXXXX 20XX, Accepted Xth XXXXXXXXXXXX 20XX

First published on the web Xth XXXXXXXXXXXX 20XX

DOI: 10.1039/b000000x

The failure to develop a degenerate, wide band gap, *p*-type oxide material has been a stumbling block for the optoelectronics industry for decades. Mg-doped LaCuOSe has recently emerged as a very promising *p*-type anode layer for optoelectronic devices, displaying high conductivities and low hole injection barriers. Despite these promising results, many questions regarding the defect chemistry of this system remain unanswered, namely (i) why does this *degenerate* semiconductor not display a Moss-Burnstein shift?, (ii) what is the origin of conductivity in doped and un-doped samples?, and (iii) why is Mg reported to be the best dopant, despite the large cation size mismatch between Mg and La? In this article we use screened hybrid density functional theory to study both intrinsic and extrinsic defects in LaCuOSe, and identify for the first time the source of charge carriers in this system. We successfully explain why LaCuOSe does not exhibit a Moss-Burstein shift, and we identify the source of the subgap optical absorption reported in experiments. Lastly we demonstrate that Mg doping *is not* the most efficient mechanism for *p*-type doping LaCuOSe, and propose an experimental reinvestigation of this system.

1 Introduction

Transparent conducting oxides (TCOs) are fascinating materials, combining the normally mutually exclusive properties of optical conductivity and high conductivity in a single material.^{1,2} TCOs play an important role the optoelectronics industry, with applications as low-emissivity windows, invisible security circuits, and as the transparent top electrode in solar cells and flat-panel displays.³ Typically, the industry standard TCOs are limited to the post transition metal oxides, such as ZnO, In₂O₃ and SnO₂,² where the ionic character of these oxides produces an oxygen 2*p* derived valence band maximum (VBM) and metal 4*s* derived conduction band maximum (CBM), resulting in large *optical* band gaps (greater than 3 eV) and excellent *n*-type conductivity when donor doped. The development of high performance *p*-type TCOs, however, has proven substantially more difficult,⁴ and is currently one of the grand challenges of materials science.⁵ The discovery of a viable *p*-type TCO would extend the utility and applications of TCOs beyond their current limitations as transparent electrodes,^{3,6} facilitating the fabrication of *p*-*n* junctions, and opening up the possibility of “transparent electronics”.⁷

For many decades researchers have attempted to invert the doping polarity of the natively *n*-type TCOs such as ZnO,

In₂O₃ and SnO₂.^{8–12} The rationale behind this strategy to design *p*-type TCOs is relatively straightforward, i.e. a *p*-type ZnO would easily be combined with *n*-type ZnO to form a *p*-*n* homo-junction, increasing the ease of device fabrication. In practice, however, a *p*-type ZnO or SnO₂ with reasonable conductivity has not been realised.^{8–12} Recent theoretical calculations have revealed that the failure to successfully invert the doping polarity of this class of material can be explained by the fact holes in these system are spontaneously compensated by the formation of ionic donor defects under all conditions,^{13,14} indicating that these *n*-type TCOs cannot be made *p*-type under equilibrium conditions.

The first truly native *p*-type TCO was reported as recently as 1997 by Hosono and co-workers,¹⁵ who found that thin films of delafossite structured CuAlO₂ displayed concomitant *native p*-type conductivity and transparency. CuAlO₂, which can be thought of as an alloy of Cu₂O and Al₂O₃, retains the valence band (VB) feature of natively *p*-type Cu₂O, where the Cu 3*d*¹⁰ states mix with the O 2*p* states.¹⁶ This raises the VB relative to the binary *n*-type TCOs,^{17–21} facilitating ease of hole formation. Hosono and co-workers then exploited the design principles that emerged from this study, subsequently called “Chemical Modulation of the Valence Band” (CMVB) to show that other Cu^I based oxides were also *p*-type TCOs, e.g. delafossite structured CuMO₂, (M = Cr, B, Sc, Y, In, Ga)^{17–24} and SrCu₂O₂.^{25–28}

It has become increasingly clear, however, that *all* of these materials are limited by poor conductivities caused by deep acceptor levels,^{29–31} and that the majority of Cu^I based ox-

^a University College London, Kathleen Lonsdale Materials Chemistry, 20 Gordon Street, London WC1H 0AJ, United Kingdom. E-mail: allenje@tcd.ie; watsong@tcd.ie

^b Diamond Light Source Ltd., Diamond House, Harwell Science and Innovation Campus, Didcot, Oxfordshire OX11 0DE, UK

^c School of Chemistry and CRANN, Trinity College Dublin, Dublin 2, Ireland

ides TCOs possess indirect band-gaps,³² which are not ideal for device performance.³³ Interest in Cu^I-based oxides for TCO applications is continuing,^{34,35} despite these material constraints.

Hosono and co-workers subsequently extended the concept of CMVB to the mixing of Cu^I state with other chalcogens such as S, Se and Te *p* states at the VBM.³⁶ In general, binary Cu₂Ch (Ch = S, Se, Te) materials display greater hole mobility than Cu₂O due to stronger hybridization of the chalcogens with the Cu 3*d* states at the VBM, but with much narrower band-gaps than oxides,³⁷ Layered oxychalcogenides, however, have emerged as attractive alternative TCOs, as they can maintain the wide band-gaps of the oxides, allied with the increased hybridization of the chalcogen, Ch *p*⁶ (Ch = S, Se, Te) and Cu 3*d*¹⁰ states at the VBM. These materials possess oxide layers with ionic cations (e.g. La, Sr etc.) sandwiched between [Cu₂Ch₂]²⁻ layers, with the Cu–Ch bonds forming VBMs with increased hybridization relative to the Cu–O VBMs in Cu^I based TCOs.³⁸

The first layered oxychalcogenide identified as a *p*-type TCO was LaCuOS, which was synthesized by Hosono and co-workers in 2000.³⁹ This layered material possessed a bandgap of 3.1 eV and when Sr doped showed *p*-type conductivity of $2.6 \times 10^{-1} \text{ S cm}^{-1}$.⁴⁰ Recently [Cu₂S₂][Sr₃Sc₂O₅] was found to have possess a band gap of 3.1 eV, coupled with an undoped *p*-type conductivity measured at 2.8 S cm^{-1} , which is higher than the best undoped delafossite system (CuBO₂, 1.65 S cm^{-1}),^{41,42} and is two orders of magnitude higher than undoped LaCuOS ($0.01 - 0.1 \text{ S cm}^{-1}$).⁴³ Interestingly, the carrier concentration in undoped [Cu₂S₂][Sr₃Sc₂O₅] is relatively low at $1 \times 10^{17} \text{ cm}^{-3}$,⁴³ which makes the high undoped conductivity relative to other Cu^I materials quite remarkable. A possible explanation for this is the extremely high hole mobility of [Cu₂S₂][Sr₃Sc₂O₅], which at $150 \text{ cm}^2 \text{ V}^{-1} \text{ s}^{-1}$ at room temperature, is the largest hole mobility of any *p*-type TCO, and also is bigger than the highest mobility reported for *n*-type TCOs (In₂O₃:Mo, $130 \text{ cm}^2 \text{ V}^{-1} \text{ s}^{-1}$).⁴³ These results indicate, however, the ability of chalcogen anions, allied with Cu^I cations to be good candidate *p*-type materials. The challenge remains to engineer a layered oxychalcogenide with sufficient *p*-type conductivity and better transparency, to equal the performance of the *n*-type TCOs.

Replacement of the chalcogen in the structure with Se results in a *p*-type material with increased conductivity, but a decreased bandgap.⁴⁴ In fact Mg-doped LaCuOSe displayed a very promising conductivity of 910 S cm^{-1} , a hole concentration greater than 10^{21} cm^{-3} and hole mobilities as high as $3.5 \text{ cm}^2 \text{ V}^{-1} \text{ s}^{-1}$.⁴⁵ However the optical band-gap of this material is only 2.8 eV, meaning that the band gap is $\sim 0.3 \text{ eV}$ too small for it to be classified possible transparent conductor.⁴⁵

Hiramatsu *et al.* proposed that a *p*-type degenerate TCO

should experience a Moss-Burstein (MB) shift (a blue shift of the optical absorption due to the fermi level being resonant inside the valence/conduction bands^{46,47}), opening up the optical band gap, and possibly moving the material to the verge of transparency⁴⁸ To date, however, LaCuOSe:Mg has never exhibited an MB shift in experiments. Indeed, optical experiments have reported sub band gap absorptions, which to date have remained of questionable origin.⁴⁸

Another puzzling question is why Mg is the optimal dopant for this system? From a cation radius perspective, Ca and Sr should be much more suitable dopants to substitute for La, yet in experiment they do not perform as well as Mg.⁴⁹ One explanation that has emerged from a recent study by Hosono and co-workers is that V_{Cu} is the likely origin of the *p*-type conductivity, with Mg-doping not increasing the number of hole carriers in this system.⁴⁸ This explanation, however, cannot explain why only Mg-doped samples can sustain the highest *p*-type carrier concentrations. In addition, this joint theory and experimental paper suggested that V_{Cu} formation is spontaneous in LaCuOSe,⁴⁸ which is highly unlikely.

In this article, we study the defect chemistry of LaCuOSe using state-of-the-art hybrid density functional theory in order to answer some of the remaining key questions relating to the *p*-type ability of this material. We specifically address: (a) the absence of a Moss-Burstein shift in optical experiments on heavily doped samples, (b) the origin of conductivity in both doped and un-doped samples, and (c) which group 2 dopant will be the most effective at generating hole carriers. In light of these results we critically discuss the previous experimental and theoretical findings.

2 Methodology

All calculations were performed using the periodic DFT code VASP,^{50,51} in which a plane-wave basis set describes the valence electronic states. The Perdew-Burke-Ernzerhof⁵² (PBE) gradient corrected functional was used to treat the exchange and correlation. The projector-augmented wave^{53,54} (PAW) method was used to describe the interactions between the cores (La:[Kr], Cu:[Ar], O:[He] and Se:[Ar]) and the valence electrons. To counteract the self interaction error and the band gap errors inherent to standard DFT functionals such as the PBE functional, higher levels of theory must be used. In this study we have used the screened hybrid density functional developed by Heyd, Scuzeria and Ernzerhof (HSE06)^{55,56}, as implemented in the VASP code.⁵⁷ HSE06 has been shown to yield improved descriptions of structure, band gap and defect properties of a number of oxide semiconductors.^{29,58–70}

Structural optimizations of bulk LaCuOSe were performed using HSE06 at a series of volumes in order to calculate the equilibrium lattice parameters. In each case the the atomic positions, lattice vector and cell angle were allowed to relax,

while the total volume was held constant. The resulting energy volume curves were fitted to the Murnaghan equation of state to obtain the equilibrium bulk cell volume.⁷¹ This approach minimizes the problems of Pulay stress and changes in basis set which can accompany volume changes in plane wave calculations. Convergence with respect to k -point sampling and plane wave energy cut off were checked, and a cutoff of 400 eV and a k -point sampling of $8 \times 8 \times 8$ were found to be sufficient. Calculations were deemed to be converged when the forces on all the atoms were less than 0.01 eV \AA^{-1} . A $3 \times 3 \times 1$ simulation cell consisting of 72 atoms was used for our defect calculations

The formation energy of a defect determines its equilibrium concentration. For defect D in charge state q the formation energy is given by

$$\Delta H_f(D, q) = (E^{D,q} - E^H) + \sum_i n_i (E_i + \mu_i) + q (E_{Fermi}^H + \epsilon_{VBM}^H) + E_{align}[q] \quad (1)$$

Where E^H is the energy of the pure host supercell, $E^{D,q}$ is the energy of the defective cell. E_i corresponds to elemental reference energies, i.e. $\text{Cu}_{(s)}$, $\text{La}_{(s)}$, $\text{Se}_{(s)}$ and $\text{O}_{2(g)}$, μ_i is the chemical potential of the species in question, and n is the number of atoms added to or taken from an external reservoir.⁷² Electrons are exchanged with the Fermi level (E_F), which ranges from the VBM ($E_F = 0 \text{ eV}$) to the calculated CBM. ϵ_{VBM}^H is the VBM eigenvalue of the host bulk and $E_{align}[q]$ is a correction used to align the VBM of the bulk and the defective supercells and also to correct for finite-size effects in the calculations of charged defects, performed using the freely available SXDEFECTALIGN code.⁷³ These finite-size effect corrections are necessary as the charge introduced into a cell can cause a spurious interaction with its periodic image, which can affect the energetics.⁷³ An additional correction was made in order to account for band-filling effects.^{74,75} The thermodynamic transition levels (ionization levels) of a given defect, $\epsilon_D(q/q')$, correspond to the Fermi-level positions at which a given defect changes from charge state q to q' :

$$\epsilon_D(q/q') = \frac{\Delta H_f(D, q) - \Delta H_f(D, q')}{q' - q} \quad (2)$$

3 Results

3.1 Geometry and Electronic structure

The HSE06 calculated a and c lattice parameters for LaCuOSe are 4.065 \AA and 8.806 \AA respectively. The HSE06 structure shows excellent agreement (within 0.1 %) with respect to the experimental values.⁷⁶ The HSE06 calculated band structure for LaCuOSe is shown in Figure 1. The valence band maximum (VBM) and conduction band minimum (CBM) both occur at the Γ point, resulting in a fundamental band gap of

2.72 eV , which is in very good agreement with the experimentally measured gap of 2.80 eV .⁷⁷ The VBM is dominated by Cu d states mixing with Se p states, as expected from the CMVB, producing a VBM effective mass in the Γ -M direction of $0.30 m_e$.

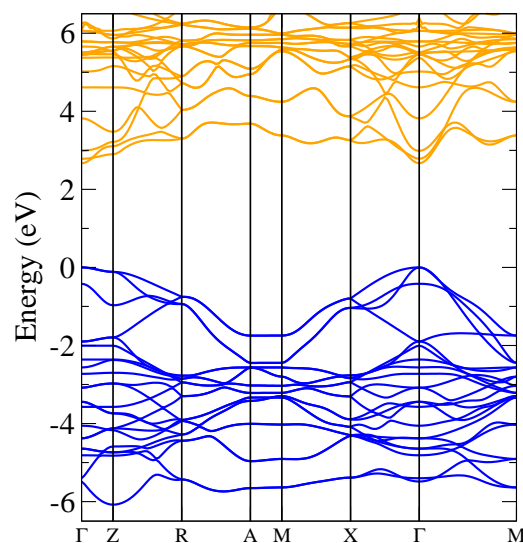


Fig. 1 HSE06 calculated band structure for LaCuOSe. The occupied valence bands and unoccupied conduction bands are coloured blue and orange respectively. The VBM is set to 0 eV.

3.2 Thermodynamic stability of LaCuOSe

Varying the chemical potentials, μ_i (see Equation 1, Theoretical Methods section), relates to varying the partial pressures experimentally. They can thus be used to set the different conditions under which LaCuOSe may form, and determine the optimum conditions for defect formation, within the global constraint of the calculated enthalpy of the host, in this instance LaCuOSe: $\mu_{\text{La}} + \mu_{\text{Cu}} + \mu_{\text{O}} + \mu_{\text{Se}} = \Delta H_f^{\text{LaCuOSe}} = -9.55 \text{ eV}$. To avoid precipitation into solid elemental La, Cu, Se and O_2 gas we also require: $\mu_{\text{La}} \leq 0$, $\mu_{\text{Cu}} \leq 0$, $\mu_{\text{O}} \leq 0$, and $\mu_{\text{Se}} \leq 0$. The chemical potentials are further constrained by the decomposition of LaCuOSe into competing binary, ternary and quaternary compounds. As LaCuOSe is a quaternary material, the complexity and number of limiting phases that need to be addressed is significantly higher than for ternary semiconductors,^{78,79} and so we have calculated the formation energy of 22 possible limiting phases: LaCu_2 , LaCu_5 , SeO_2 , Se_2O_5 , La_2O_3 , CuO , Cu_2O , CuSe , Cu_2Se , Cu_3Se_2 , CuSe_2 , La_3Se_4 , LaSe , LaSe_2 , CuLaO_2 , CuLaSe_2 , La_2CuO_4 , LaCuO_3 , CuSe_2O_5 , La_2SeO_2 , $\text{La}_4\text{Se}_3\text{O}_4$, $\text{La}_2(\text{SeO}_3)_3$, $\text{La}(\text{CuO}_2)_2$, and $\text{La}_2\text{Cu}(\text{SeO}_3)_4$. Previous DFT defect studies of LaCuOSe have failed to take the

formation of competing phases into account, meaning their defect energetics are probably for an unphysical conditions.^{48,80} Following the standard approach,^{29,81,82} the phase diagram for LaCuOSe was computed using the CPLAP (Chemical Potential Limits Analysis Program),⁸³ taking into account the limitations caused by formation of the competing phases. The stable polyhedron formed by LaCuOSe under these limitations is plotted in Figure 2. Our analysis indicates that the limiting phases are: CuLaO_2 , La_2O_3 , La_3Se_4 , LaCuSe_2 , Cu_2Se , Cu_3Se_2 , La_2SeO_2 , $\text{La}_2(\text{SeO}_3)_3$, $\text{La}_4\text{Se}_3\text{O}_4$, and LaCu_5 . From this analysis, we have identified 20 representative chemical-potential-points, which are intersections of the limiting phases. The chemical potentials at the 20 individual intersection points are listed elsewhere.⁸³ This highlights the fact that although quaternary materials exhibit more flexibility for property tuning than binary and ternary systems, secondary phases also become more competitive, and care needs to be taken when growing quaternary systems.

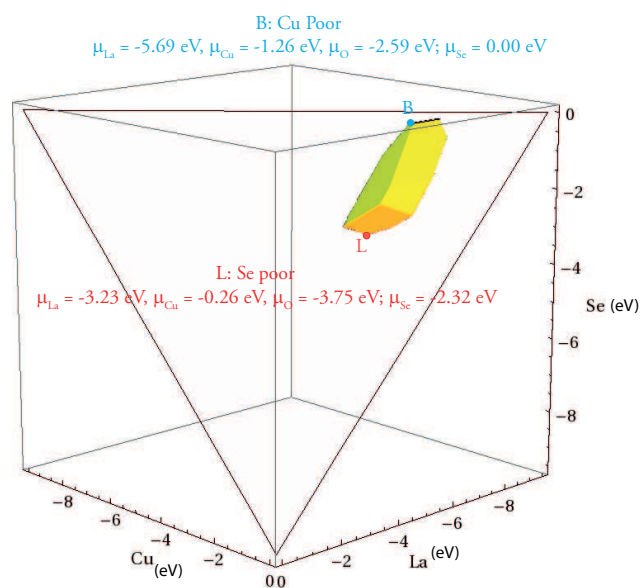


Fig. 2 Illustration of the accessible (μ_{Se} , μ_{Cu} , μ_{La}) chemical potential range. The polyhedra vertices are determined by the formation enthalpy of LaCuOSe. Limits imposed by the formation of competing binary, ternary and quaternary compounds result in the stable region shaded yellow. Environments B and L are indicated by the blue and red spheres.

3.3 Intrinsic Defects

Figure 3 displays the range of neutral formation energies for all the possible intrinsic defects in LaCuOSe at the 20 chemical potential limits that we have selected. It is clear that the formation energy of the defects can vary greatly, depending on

the growth environments. It is also clear that at some growth environments (e.g. F, H, J, L, O, P and T), formation of the n -type defect V_{Se} , is favoured over all native p -type defects, which would not be ideal for high performance samples.

To analyse the effect of growth environment on the p -type ability of *undoped* LaCuOSe samples, we have chosen two representative chemical potential limits: (i) Environment B, where the neutral formation energy of the V_{Cu} is lowest and represents Se-rich, La poor and Cu-poor growth conditions, and (ii) environment L where the V_{Se} is the dominant neutral defect, which represents Se-poor, O-poor, and relatively La-rich and Cu-rich conditions, as indicated in Figure 2.

A plot of formation energy as a function of Fermi-level position for all intrinsic defects in LaCuOSe for both growth environment A and L is displayed in Figure 4. For environment B, it is clear that the V_{Cu} is the dominant acceptor defect, with a formation energy of 1.45 eV, and it behaves as a relatively shallow acceptor, with a $0/-1$ transition (ionization) level at approximately 114 meV above the VBM. The V_{Cu} is not compensated by any other defects over the entire range of the band gap, indicating that under growth condition B, the material will be p -type in nature, with no “hole-killing” defects present. It should be noted that although “self-doping” by cation-on-cation antisites can dominate conductivity in other multi-ternary systems,^{29,84–87} in LaCuOSe both the Cu_{La} and La_{Cu} antisites are quite high in energy and the concentration of antisite defects in LaCuOSe is expected to be negligible under equilibrium conditions.

Interestingly, the V_{Se} is found to be an *ultra* deep donor, and also a negative- U type defect, possessing a $+2/0$ transition level at 210 meV above the VBM (or ~ 2.5 eV below the CBM). The $+2$ and $+1$ charge states of the V_{O} are found to be stable, which is quite unusual, as in the majority of wide band gap oxides, V_{O} is a negative- U type defect, with only the $+2$ and neutral charge states stable within the band gap.^{11,88–94}

When considering the behaviour of anion vacancies in this system, it is useful to think about an anion vacancy in terms of Kröger-Vink notation, i.e. $[V_{\text{anion}}^{\bullet\bullet} + 2e]$ which means that there is a doubly charged vacancy on an anion site, plus two free electrons. A doubly occupied vacancy would be expected to *repel* the neighbouring positively charged cations, however, for the V_{Se} the cations move towards the vacancy site, Figure 5 (a), indicating that significant negative charge exists in the vacancy site. This is explained by the fact that the electrons are trapped in the V_{Se} , in an F-centre like fashion, complete with polaronic distortion. For the V_{Se}^{+2} , the two electrons are now absent from the vacancy, and the Cu ions are strongly repelled away from the vacancy site, Figure 5 (c). It is the large relaxations experienced by the 0 and $+2$ charge states which stabilize these charge states relative to the $+1$ charge state, making the V_{Se} a negative- U centre in LaCuOSe. This behaviour is consistent with that of the V_{O} in ZnO and related wide band

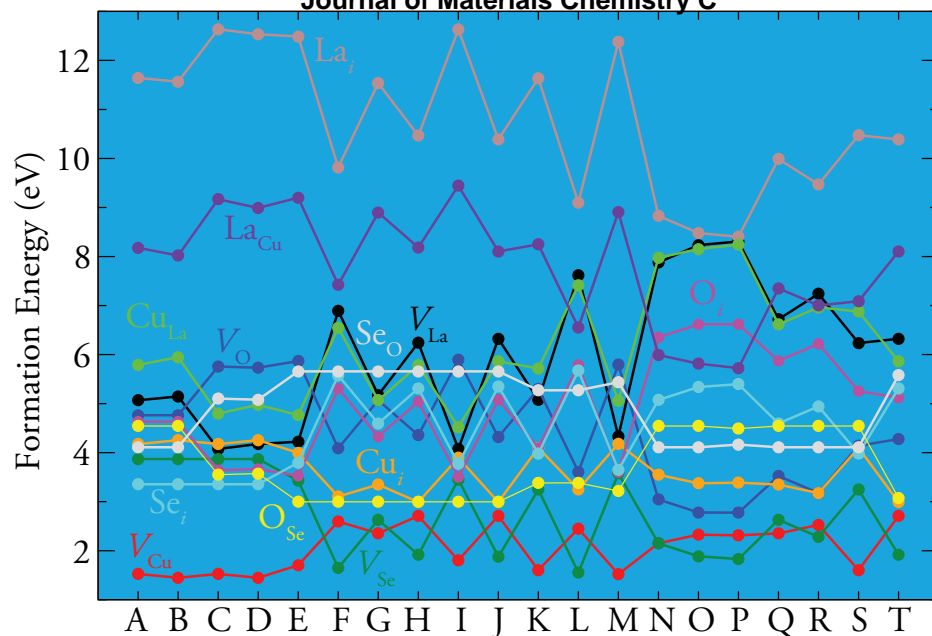


Fig. 3 Formation energy of all defects considered in LaCuOSe in the neutral charge state at the 20 chemical potential limits from Figure 2.

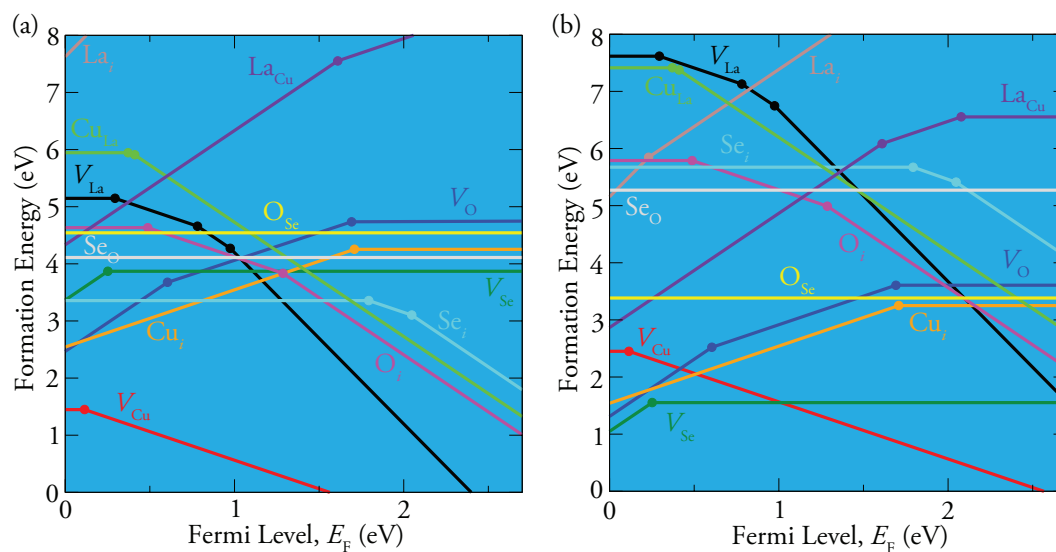


Fig. 4 Formation energies for intrinsic defects in LaCuOSe under the conditions B (a) and L (b) chosen in Figure 2. The slope of the lines denote the charge state, the larger the slope, the bigger the charge state. The solid dots represent the transition levels ϵ (q/qt).

gap oxides, where V_O is a well characterized negative- U type defect.

For the V_O in LaCuOSe, the neighbouring La ions are not attracted towards the vacancy position, and in fact are slightly repelled, with the La ions distorting away from the vacancy

by $\sim 2.7\%$. Subsequent relaxations of the +1 and then the +2 charge state cause relaxations of the La ions outward by $\sim 2.2\%$ and $\sim 4.1\%$ respectively, Figure 5 (d-e). These relaxations are not large enough to stabilize a negative- U type behaviour. This type of behaviour has been previously noted

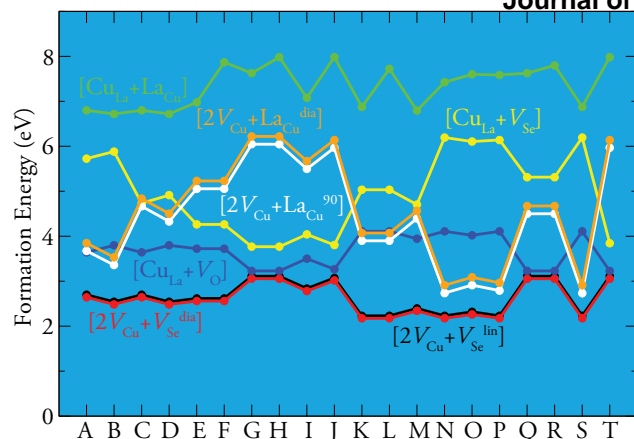


Fig. 6 Formation energy of all 7 complexes considered in LaCuOSe in the neutral charge state at environment B from 2.

for small band gap oxides,^{95–97} but never for a wide band gap oxide.

Under Se-poor/O-poor growth conditions (environment L), the defect landscape is very different. For E_F close to the VBM, the formation energy of both the V_{Se} and the V_O in their +2 charge states, and Cu_i in the +1 charge state dominate, indicating that p -type conductivity will be full compensated by n -type defects. For E_F above ~ 1 eV above the VBM, V_{Cu}^{-1} dominates, indicating that n -type conductivity is also fully compensated. Therefore under Se-poor/O-poor conditions, E_F will be trapped in the band gap, limiting any conductivity.

3.4 Intrinsic Defect Complexes

The formation of charge compensated defect complexes are prevalent in some ternary and quaternary Cu^I -based materials. In solar cell absorbers such as $CuInSe_2$ ⁹⁸ or CZTS^{99,100}, these electrically benign complexes are advantageous, but in LaCuOSe, any complexes formed with the V_{Cu} , for example, would kill conductivity, hampering its use as a p -type anode layer, or as a thermoelectric material. In Table 1, we list the formation energy of 7 defect complexes which could plausibly form.

We define three formation energies: (i) $\Delta H_{separated}$, which is the sum of the individual formation energies of these non-interacting, isolated single defects that make up the complex, (ii) $\Delta H_{complex}$, which is the formation energy of the complex, and (iii) ΔH_{int} , the interaction energy, which is the difference in formation energy between $\Delta H_{separated}$ and $\Delta H_{complex}$. Thus, ΔH_{int} demonstrates the driving force for complex formation. The formation energy of the defect complexes ($\Delta H_{complex}$) are displayed in Figure 6.

ΔH_{int} can be influenced by many factors, as the formation energy of a complex can be determined by contributions such as (a) charge compensation, i.e. charge transfer between neutral donors to neutral acceptors, (b) Coulomb attraction between charged donors and charged acceptors, and (c) strain relief.⁹⁸ In practice, the contribution from charge transfer can be as much as the magnitude of the band gap, i.e. an electron occupying a high donor level near the CBM transferring to a low-lying acceptor level near the VBM. From Table 1, we can see that although ΔH_{int} is large for these complexes, $\Delta H_{complex}$ is quite big in all cases, indicating that these complexes should not have a high population in LaCuOSe crystals.

3.5 Extrinsic Acceptor Dopants

As the thermodynamics of acceptor doping of LaCuOSe are so poorly understood, we have studied Mg-, Ca- and Sr-doped LaCuOSe, with the results shown in Figure 7. We also present results for Zn doping, in an attempt to identify a donor dopant which could make this material bipolar. Our results clearly show that Sr_{La} is the lowest energy acceptor, and is not compensated by the formation of Sr_{Cu} or Sr_i . The formation energy of Sr_{La} is lower than that of the V_{Cu} , indicating that Sr doping will significantly increase the hole concentration in LaCuOSe. Mg-doping, on the other hand, is much higher in energy, indicating that it will not increase the hole concentration significantly. This is consistent with recent reports that the hole concentration does not change upon Mg doping, and that the origin of the conductivity in Mg-doped LaCuOSe is the V_{Cu} .⁴⁸ It does not explain, however, why undoped samples do not display more degenerate behaviour.⁴⁸ The trend in solubility of acceptor dopants in LaCuOSe follows that expected based on size effects, with the Sr < Ca < Mg.

To address the possibility that acceptors in Ca- and Sr-doped LaCuOSe could somehow be passivated by intrinsic defect complexes, we have also investigated the possibility that a complex of $[M_{La} + V_O]$ could form, with the results presented in Figure 7. The formation of $[M_{La} + V_O]$ complexes will not compensate the formation of M_{La} for any of the group 2 dopants under typical p -type conditions. Thus ionic compensation is unlikely to affect negatively the p -type abilities of Ca- and Sr-doped LaCuOSe relative to Mg-LaCuOSe.

Zn self compensates in LaCuOSe, with the Zn_{La} and Zn_{Cu} crossing over in the band gap, effectively trapping the Fermi level at the cross over, although under anion-rich conditions, Zn-doping on the Cu site could drive the Fermi level towards mid gap, where it will be compensated by the V_{Cu} in the -1 charge state, Figure 7 (b).

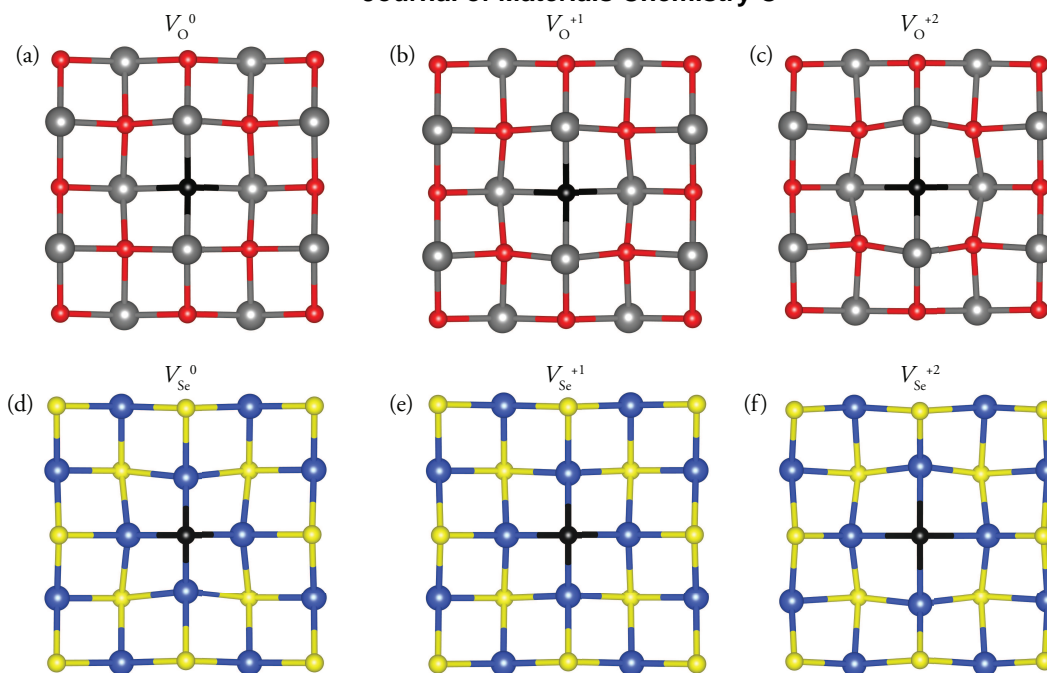


Fig. 5 (a)-(c) Top view of the geometry around a relaxed V_{Se} in a $[Cu_2Se_2]^{2-}$ layer in the (a) neutral, (b) +1 and (c) +2 charge states. (d)-(f) Top view of the geometry around a relaxed V_O in a $[La_2O_2]^{2+}$ layer in the (a) neutral, (b) +1 and (c) +2 charge states. Yellow, blue, red and grey spheres denote Se, Cu, O and La respectively. In all cases the position of the vacancy is denoted by a black sphere.

Table 1 The calculated formation energy, $\Delta H_{separated}$, of noninteracting neutral defects, the interaction energy ΔH_{int} , and the formation energy of the complex $\Delta H_{complex}$ at chemical potential point B, i.e. $\Delta H_{int} = \Delta H_{separated} - \Delta H_{complex}$. All energies are given in eV.

Complexes	$2V_{Cu} + V_{Se}^{ang}$	$2V_{Cu} + V_{Se}^{lin}$	$Cu_{La} + La_{Cu}$	$Cu_{La} + V_O$	$Cu_{La} + V_{Se}$	$2V_{Cu} + La_{Cu}^{diag}$	$2V_{Cu} + La_{Cu}^{90}$
$\Delta H_{separated}$	6.92	6.92	13.96	10.55	9.65	11.22	11.23
ΔH_{int}	-4.23	-4.27	-7.17	-6.91	-3.93	-7.38	-7.56
$\Delta H_{complex}$	2.69	2.64	6.79	3.64	5.72	3.84	3.67

4 Discussion

Our results clearly show that the growth conditions can have a large effect on the conductivity trends. If grown in unsuitable growth conditions (i.e. metal-rich/anion-poor), native donors become more populous, and will kill p -type conductivity.

Under ideal p -type conditions, V_{Cu} is the dominant acceptor defect, and with its relatively shallow ionization levels, will ensure reasonable p -type conductivity. It should be noted that the energy needed to ionize V_{Cu} in LaCuOSe is far less than that seen for the delafossite structured Cu^I -based TCOs, e.g. $CuAlO_2$ (0.68 eV)²⁹ and $CuCrO_2$ (0.37 eV).¹⁰¹ This is a direct consequence of the dual effect of the Cu–Se mixing at the VBM raising the VBM and ensuring a less deep acceptor level.

Sr is the most soluble acceptor dopant in LaCuOSe, followed by Ca and then Mg, which is to be expected based on ionic-radii arguments. This is consistent with the performance of group 2 dopants in bulk samples,⁴⁹ but is at variance with the conductivity trends for epitaxial thin films.⁴⁹ It remains unclear why Mg has been found to be the best dopants for producing highly degenerate LaCuOSe,¹⁰² but our analysis indicate that Sr *should* be the optimal dopant. Under cation-poor/anion-rich conditions, Sr_{La} will significantly enhance to concentration of free holes in the system, as its formation energy is significantly less than that of V_{Cu} . Therefore, we propose that the acceptor doping of LaCuOSe thin films needs to be experimentally reinvestigated, so the full potential of this material can be realised.

Heavily doped LaCuOSe is routinely described as a degen-

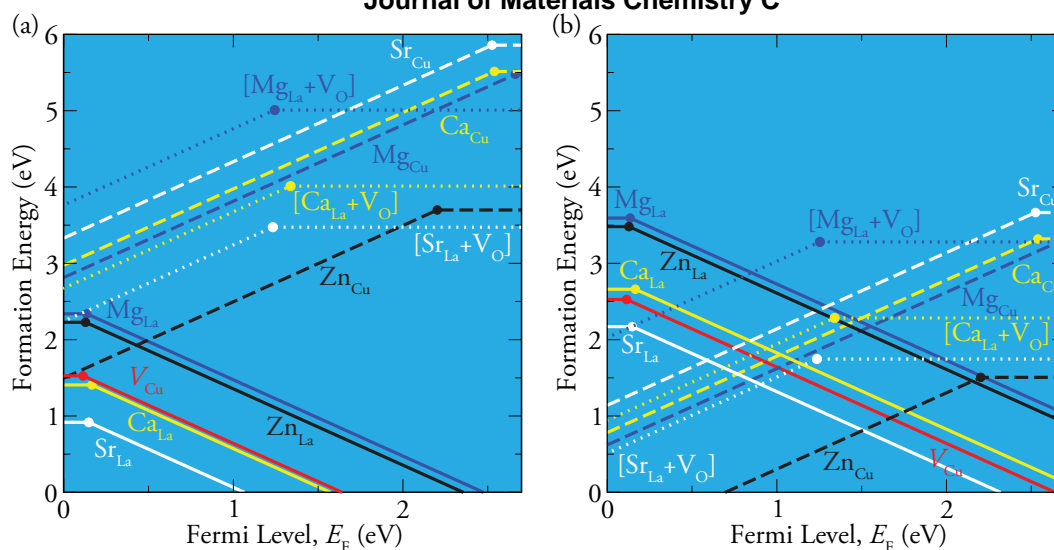


Fig. 7 Formation energies for extrinsic defects in LaCuOSe under the conditions B (a) and L (b) chosen in Figure 2. The slope of the lines denote the charge state, the larger the slope, the bigger the charge state. The solid dots represent the transition levels $\epsilon(q/q')$.

erate semiconductor; however, it does not display a Moss-Burstein (blue shift) shift of the optical band gap when acceptor doped.⁸⁰ In fact, in the optical spectra, sub-band gap absorption is observed, with a broad peak appearing from the VBM to ~ 0.6 eV above the VBM. Previous theoretical assessments of the defect chemistry of LaCuOSe have yielded metallic descriptions of the V_{Cu} and V_{La} , and have concluded that they are the source of the degenerate conductivity.⁸⁰ These studies, however, have assumed that the PBE functional, which typically erroneously delocalizes defect states in Cu-based materials,^{67,103} is sufficient. This assumption, allied to the failure to account for competing chemical potential limits, leads to the unfortunate conclusion that these defect are resonant in the VB, and that the formation energy of V_{Cu} is in fact spontaneous. If V_{Cu} formation were spontaneous and resulted in metallic conductivity in LaCuOSe, the concentration of charge carriers in nominally undoped samples would be expected to be far higher than reported,⁸⁰ and heavy acceptor doping to achieve a degenerate semiconducting state would not be necessary.⁴⁸

The inappropriate use of the PBE functional has led to the identification of the $[V_{Cu} + V_{Se}]$ complex as the likely source of sub band gap absorption seen in experiments.⁴⁸ In fact $[V_{Cu} + V_{Se}]$ would act as a donor, and so would be very unlikely to produce hole states above the VBM. By analysing the optical transition levels (OTLs) of the lowest energy defects in LaCuOSe, we found that the 0/-1 OTL for V_{Cu} is situated at 0.24 eV above the VBM, in reasonable agreement with experiment. In addition, while a large optical band gap is vi-

tal for a material to be transparent, *p*-TCO materials should also have no visible light absorption between the VBM and the bands below.²⁵ This caveat is similar to that for *n*-type TCOs, where there should be no absorption between the CBM and the conduction bands above.¹⁰⁴ For *p*-type (*n*-type) TCOs, it is necessary to avoid transitions between unoccupied (occupied) defect bands and the bands within 3.1 eV of the VBM (CBM), meaning that the defective systems are still transparent to visible light.¹⁰⁴

Acceptor defects in LaCuOSe do not move the Fermi level into the valence band, and it is apparent that transitions from the valence band to the defect state are permitted, as can clearly be seen in the experimental absorption spectra.⁴⁸ Thus LaCuOSe cannot be expected to experience a Moss-Burstein shift, and so the optical band gap can not be increased by acceptor doping. As both native and acceptor dopant defects in LaCuOSe cause defect levels *above* the VBM, however, it is still unclear why LaCuOSe doped with Mg displays degenerate semiconductor behaviour.

What is clear, however, is that Mg is not the optimum dopant for enhancing the hole carrier concentration in LaCuOSe, and that Sr doping represents the best option. An experimental reinvestigation of acceptor doping of LaCuOSe in thin films is therefore clearly warranted. Nevertheless, our results explain the increased performance of LaCuOSe over other Cu^I-O based wide band gap materials, and present a blueprint for the further optimization of LaCuOSe for device applications.

The behaviour of both intrinsic and extrinsic defects in LaCuOSe has been investigated using hybrid density functional theory. The importance of correctly analysing the thermodynamic stability of the material of interest with respect to other competing phases has been demonstrated. Our results clearly show that under *p*-type growth conditions V_{Cu} will dominate, and will not be compensated by any hole killing defects. We have explained for the first time why LaCuOSe does not exhibit a Moss-Burstein shift when heavily acceptor doped, and also demonstrated that Sr, and not Mg, is the ideal dopant for acceptor doping LaCuOSe. We have also identified the possible origin of the puzzling sub band gap absorption seen in LaCuOSe samples. It is expected that the defect behaviour reported herein will be similar for other quaternary layered oxychalcogenide materials.

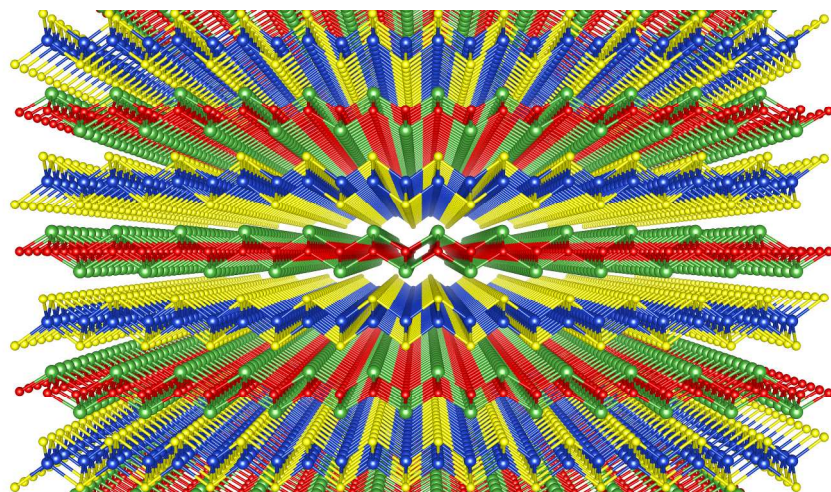
6 Acknowledgements

This work in TCD was supported by SFI through the PI programme (PI Grant numbers 06/IN.1/192 and 06/IN.1/192/EC07). Calculations in TCD were performed on the Lonsdale and Kelvin clusters as maintained by TCHPC, and the Stokes and Fionn clusters as maintained by ICHEC. The UCL/Diamond work presented here made use of the UCL Legion HPC Facility, the IRIDIS cluster provided by the EPSRC funded Centre for Innovation (EP/K000144/1 and EP/K000136/1), and the HECToR and ARCHER supercomputers through membership of the UK's HPC Materials Chemistry Consortium, which is funded by EPSRC grant EP/L000202.

References

- 1 K. Hayashi, S. Matsuishi, T. Kamiya, M. Hirano and H. Hosono, *Nature*, 2002, **419**, 462–465.
- 2 T. Minami, *Semicond. Sci. Tech.*, 2005, **20**, S35–S44.
- 3 R. G. Gordon, *MRS Bull.*, 2000, **25**, 52–57.
- 4 A. N. Banerjee and K. K. Chattopadhyay, *Prog. Cryst. Growth Char. Mater.*, 2005, **50**, 52.
- 5 G. Hautier, A. Miglio, G. Ceder, G. M. Riganese and X. Gonze, *Nat. Comm.*, 2013, **4**, 2292.
- 6 G. Thomas, *Nature*, 1997, **389**, 907.
- 7 G. Thomas, *Nature*, 1997, **389**, 907.
- 8 D. C. Look, *Semicond. Sci. Technol.*, 2005, **20**, S55–S61.
- 9 S. Lany and A. Zunger, *Phys. Rev. B*, 2009, **80**, 085202.
- 10 G. Brauer, J. Kuriplach, C. C. Ling and A. B. Djuricic, *J. Phys. Conf. Ser.*, 2011, **265**, 012002.
- 11 S. Lany and A. Zunger, *Phys. Rev. B*, 2010, **81**, 205209.
- 12 J. J. Lyons, A. Janotti and C. G. Van de Walle, *Appl. Phys. Lett.*, 2009, **95**, 252105.
- 13 D. O. Scanlon and G. W. Watson, *J. Mater. Chem.*, 2012, **22**, 25236.
- 14 C. R. A. Catlow, A. A. Sokol and A. Walsh, *Chem. Comm.*, 2011, **47**, 3386–3388.
- 15 H. Kawazoe, H. Yasakuwa, H. Hyodo, M. Kurita, H. Yanagi and H. Hosono, *Nature*, 1997, **389**, 939.
- 16 X. A. H. . M. C. Hu, Z.; Huang, *J. Phys. Chem. B*, 2008, **112**, 7837–7849.
- 17 K. Ueda, T. Hase, H. Yanagi, H. Kawazoe, H. Hosono, H. Ohta, M. Orita and M. Hirano, *J. Appl. Phys.*, 2001, **89**, 1790–1793.
- 18 H. Yanagi, T. Hase, S. Ibuki, K. Ueda and H. Hosono, *Appl. Phys. Lett.*, 2001, **78**, 1583–1585.
- 19 H. Yanagi, S.-I. Inoue, K. Ueda, H. Kawazoe, H. Hosono and N. Hamada, *J. Appl. Phys.*, 2000, **88**, 4059–4163.
- 20 X. Nie, S. H. Wei and S. B. Zhang, *Phys. Rev. Lett.*, 2002, **88**, 066405.
- 21 D. Shin, J. S. Foord, D. J. Payne, T. Arnold, D. J. Aston, R. G. Egdell, K. G. Godinho, D. O. Scanlon, B. J. Morgan, G. W. Watson, E. Mugnier, C. Yaicle, A. Rougier, P. A. Glans, L. F. J. Piper and K. E. Smith, *Phys. Rev. B*, 2009, **80**, 233105.
- 22 D. O. Scanlon, A. Walsh, B. J. Morgan, G. W. Watson, D. J. Payne and R. G. Egdell, *Phys. Rev. B*, 2009, **79**, 035101.
- 23 D. O. Scanlon, A. Walsh and G. W. Watson, *Chem. Mater.*, 2009, **21**, 4568–4576.
- 24 T. Arnold, D. J. Payne, A. Bourlange, J. P. Hu, R. G. Egdell, L. F. J. Piper, L. Colakerol, A. De Masi, P. A. Glans, T. Learmonth, K. E. Smith, J. Guo, D. O. Scanlon, A. Walsh, B. J. Morgan and G. W. Watson, *Phys. Rev. B*, 2009, **79**, 075102.
- 25 X. L. Nie, S. H. Wei and S. B. Zhang, *Phys. Rev. B*, 2002, **65**, 075111.
- 26 A. Kudo, H. Yanagi, H. Hosono and H. Kawazoe, *Appl. Phys. Lett.*, 1998, **73**, 220–222.
- 27 K. G. Godinho, G. W. Watson, A. Walsh, A. J. H. Green, D. J. Payne, J. Harmer and R. G. Egdell, *J. Mater. Chem.*, 2008, **18**, 2798–2806.
- 28 K. G. Godinho, J. J. Carey, B. J. Morgan, D. O. Scanlon and G. W. Watson, *J. Mater. Chem.*, 2010, **20**, 1086–1096.
- 29 D. O. Scanlon and G. W. Watson, *J. Phys. Chem. Lett.*, 2010, **1**, 3195–3199.
- 30 D. O. Scanlon and G. W. Watson, *J. Mater. Chem.*, 2011, **21**, 3655–3663.
- 31 J. Tate, H. L. Ju, J. C. Moon, A. Zakutayev, A. P. Richard, J. Russell and D. H. McIntyre, *Phys. Rev. B*, 2009, **80**, 165206.
- 32 D. O. Scanlon, K. G. Godinho, B. J. Morgan and G. W. Watson, *J. Chem. Phys.*, 2010, **132**, 024707.
- 33 R. W. Brander, *Rev. Phys. Technol.*, 1972, **21**, 145–194.
- 34 C. Ruttanapun, W. Prachamon and A. Wichainchai, *Curr. Appl. Phys.*, 2012, **12**, 166–170.
- 35 H. Y. Chen and J. H. Wu, *Appl. Surf. Sci.*, 2012, **258**, 4844–4847.
- 36 K. Ueda, H. Hiramatsu, M. Hirano, T. Kamiya and H. Hosono, *Thin Solid Films*, 2006, **496**, 8–15.
- 37 M. L. Liu, L. B. Wu, F. Q. Huang, L. D. Chen and J. A. Ibers, *J. Solid State Chem.*, 2007, **180**, 62–69.
- 38 S. J. Clarke, P. Adamson, S. J. C. Herkelrath, O. J. Rutt, D. R. Parker, M. J. Pitcher and C. F. Smura, *Inorg. Chem.*, 2008, **47**, 8473–8486.
- 39 K. Ueda, S. Inoue, S. Hirose, H. Kawazoe and H. Hosono, *Appl. Phys. Lett.*, 2000, **77**, 2701–2703.
- 40 H. Hiramatsu, K. Ueda, H. Ohta, M. Orita, M. Hirano and H. Hosono, *Thin Solid Films*, 2002, **411**, 125–128.
- 41 M. Snure and A. Tiwari, *Appl. Phys. Lett.*, 2007, **91**, 092123.
- 42 D. O. Scanlon and G. W. Watson, *Chem. Mater.*, 2009, **21**, 5435–5442.
- 43 M. L. Liu, L. B. Wu, F. Q. Huang, L. D. Chen and I. W. Chen, *J. Appl. Phys.*, 2007, **102**, 116108.
- 44 K. Ueda, H. Hosono and N. Hamada, *J. Phys.: Condens. Matter*, 2004, **16**, 5179–5186.
- 45 H. Hiramatsu, K. Ueda, H. Ohta, H. Hirano, M. Kikuchi, H. Yanagi, T. Kamiya and H. Hosono, *Appl. Phys. Lett.*, 2007, **91**, 012104.
- 46 T. S. Moss, *Proc. Phys. Soc. B*, 1954, **67**, 775.
- 47 E. Burstein, *Physical Review*, 1954, **93**, 632.
- 48 H. Hiramatsu, T. Kamiya, T. Tohei, E. Ikenaga, T. Mizoguchi,

- Y. Ikuhara, K. Kobayashi and H. Hosono, *J. Am. Chem. Soc.*, 2010, **132**, 15060–15067.
- 49 H. Hiramatsu, K. Ueda, H. Ohta, M. Hirano, T. Kamiya and H. Hosono, *Applied Physics Letters*, 2003, **82**, 1048.
- 50 G. Kresse and J. Furthmüller, *Phys. Rev. B*, 1996, **54**, 11169–11186.
- 51 G. Kresse and J. Hafner, *Phys. Rev. B*, 1994, **49**, 14251–14271.
- 52 K. E. M. Perdew, J.P.; Burke, *Phys. Rev. Lett.*, 1996, **77**, 3865–3868.
- 53 P. E. Blöchl, *Phys. Rev. B*, 1994, **50**, 17953.
- 54 G. Kresse and D. Joubert, *Phys. Rev. B*, 1999, **59**, 1758–1775.
- 55 S. Heyd, G. E. Scuseria and M. Ernzerhof, *J. Chem. Phys.*, 2003, **118**, 8207–8215.
- 56 A. V. Krugau, O. A. Vydrov, A. F. Izmaylov and G. E. Scuseria, *J. Chem. Phys.*, 2006, **125**, 224106.
- 57 J. Paier, M. Marsman, K. Hummer, G. Kresse, I. C. Gerber and J. G. Ángyán, *J. Chem. Phys.*, 2006, **124**, 154709–154713.
- 58 J. Heyd and G. E. Scuseria, *J. Chem. Phys.*, 2004, **121**, 1187–1192.
- 59 J. Heyd, J. E. Peralta, G. E. Scuseria and R. L. Martin, *J. Chem. Phys.*, 2005, **123**, 174101.
- 60 J. L. F. Da Silva, M. V. Ganduglia-Pirovano, J. Sauer, V. Bayer and G. Kresse, *Phys. Rev. B*, 2007, **75**, 045121.
- 61 A. Walsh, J. L. F. Da Silva, Y. Yan, M. M. Al-Jassim and S. H. Wei, *Phys. Rev. B*, 2009, **79**, 073105.
- 62 S. Chen, Z. G. Gong, A. Walsh and S. H. Wei, *Appl. Phys. Lett.*, 2009, **94**, 041903.
- 63 J. P. Allen, D. O. Scanlon and G. W. Watson, *Phys. Rev. B*, 2010, **81**, 161103(R).
- 64 B. G. Janesko, T. M. Henderson and G. E. Scuseria, *Phys. Chem. Chem. Phys.*, 2009, **11**, 443–454.
- 65 D. O. Scanlon and G. W. Watson, *J. Phys. Chem. Lett.*, 2010, **1**, 2582–2585.
- 66 J. E. Peralta, J. Heyd, G. E. Scuseria and R. L. Martin, *Phys. Rev. B*, 2006, **74**, 073101.
- 67 D. O. Scanlon, B. J. Morgan, G. W. Watson and A. Walsh, *Phys. Rev. Lett.*, 2009, **103**, 096405.
- 68 A. Stroppa and G. Kresse, *Phys. Rev. B*, 2009, **79**, 201201.
- 69 A. Stroppa and S. Picozzi, *Phys. Chem. Chem. Phys.*, 2010, **12**, 5405–5416.
- 70 D. O. Scanlon and G. W. Watson, *Phys. Rev. Lett.*, 2011, **106**, 186403.
- 71 F. D. Murnaghan, *Proc. Natl. Acad. Sci. U.S.A.*, 1944, **30**, 244–247.
- 72 C. G. Van de Walle and J. Neugebauer, *J. Appl. Phys.*, 2004, **95**, 3851–3879.
- 73 C. Freysoldt, J. Neugebauer and C. G. V. de Walle, *Phys. Rev. Lett.*, 2009, **102**, 016402.
- 74 S. Lany and A. Zunger, *Phys. Rev. B*, 2008, **78**, 235104.
- 75 A. Walsh, Y. F. Yan, M. M. Al-Jassim and S. H. Wei, *Journal of Physical Chemistry C*, 2008, **112**, 12044.
- 76 K. Ueda and H. Hosono, *Thin Solid Films*, 2002, **411**, 115–118.
- 77 K. Ueda, H. Hosono and N. Hamada, *J. Phys. Conds. Matter*, 2004, **16**, 5179–5186.
- 78 A. Zakutayev, J. Tate and G. Schneider, *Phys. Rev. B*, 2010, **82**, 195204.
- 79 S. Chen, X. G. Gong, A. Walsh and S. H. Wei, *Appl. Phys. Lett.*, 2010, **96**, 021902.
- 80 H. Hiramatsu, T. Kamiya, K. Ueda, M. Hirano and H. Hosono, *Phys. Status. Solidi.*, 2010, **207**, 1636–1641.
- 81 C. Persson, Y.-J. Zhao, S. Lany and A. Zunger, *Phys. Rev. B*, 2005, **72**, 035211.
- 82 D. O. Scanlon, P. D. C. King, A. Singh, R. P. de la Torre, G. McKeown Walker, G. Balakrishnan, F. Baumberger and C. R. A. Catlow, *Adv. Mater.*, 2012, **24**, 2154–2158.
- 83 J. Buckeridge, D. O. Scanlon, A. Walsh and C. R. A. Catlow, *Comput. Phys. Commun.*, 2014, **185**, 330–338.
- 84 H. Peng, J. H. Song, E. Mitchell Hopper, Q. Zhu, T. O. Mason and A. J. Freeman, *Chem. Mater.*, 2012, **24**, 106–114.
- 85 T. R. Paudel, A. Zakutayev, S. Lany, M. d’Avezec and A. Zunger, *Adv. Funct. Mater.*, 2011, **21**, 4493.
- 86 J. D. Perkins, T. R. Paudel, A. Zakutayev, P. Ndione, P. A. Parilla, D. L. Young, S. Lany, D. S. Ginley, A. Zunger, N. H. Perry, Y. Tang, M. Grayson, T. O. Mason, J. S. Bettinger, Y. Shi and M. F. Toney, *Phys. Rev. B*, 2011, **84**, 205207.
- 87 A. Zakutayev, T. R. Paudel, P. F. Ndione, J. D. Perkins, S. Lany, A. Zunger and D. S. Ginley, *Phys. Rev. B*, 2012, **85**, 085204.
- 88 S. Lany and A. Zunger, *Phys. Rev. B*, 2008, **78**, 235104.
- 89 A. Janotti and C. G. Van de Walle, *App. Phys. Lett.*, 2005, **87**, 122102.
- 90 F. Oba, A. Togo, I. Tanaka, J. Paier and G. Kresse, *Phys. Rev. B*, 2008, **77**, 245202.
- 91 A. K. Singh, A. Janotti, M. Scheffler and C. G. Van de Walle, *Phys. Rev. Lett.*, 2008, **101**, 055502–4.
- 92 J. B. Varley, J. R. Weber, A. Janotti and C. G. V. de Walle, *Appl. Phys. Lett.*, 2010, **97**, 142106.
- 93 P. Agoston, K. Albe, R. M. Nieminen and M. J. Piska, *Phys. Rev. Lett.*, 2009, **103**, 245501.
- 94 S. Limpijumngong, P. Reunchan, A. Janotti and C. G. Van de Walle, *Phys. Rev. B*, 2009, **80**, 193202.
- 95 M. Burbano, D. O. Scanlon and G. W. Watson, *J. Am. Chem. Soc.*, 2011, **133**, 15065–15072.
- 96 A. B. Kehoe, D. O. Scanlon and G. W. Watson, *Phys. Rev. B*, 2011, **83**, 233202.
- 97 D. O. Scanlon, A. B. Kehoe, G. W. Watson, M. O. Jones, W. I. F. David, D. J. Payne, R. J. Egdel, P. P. Edwards and A. Walsh, *Phys. Rev. Lett.*, 2011, **107**, 246402.
- 98 S. B. Zhang, S. H. Wei, A. Zunger and H. Katayama-Yoshida, *Phys. Rev. B*, 1998, **57**, 9642–9656.
- 99 S. Chen, A. Walsh, X. G. Gong and S. H. Wei, *Adv. Mater.*, 2013, **25**, 1522–1539.
- 100 S. Chen, J. H. Yang, X. G. Gong, A. Walsh and S. H. Wei, *Phys. Rev. B*, 2010, **81**, 245204.
- 101 D. O. Scanlon and G. W. Watson, *J. Mater. Chem.*, 2011, **21**, 3655.
- 102 H. Hiramatsu, K. Ueda, H. Ohta, M. Hirano, T. Kamiya and H. Hosono, *Thin Solid Films*, 2003, **445**, 304.
- 103 D. O. Scanlon, B. J. Morgan and G. W. Watson, *J. Chem. Phys.*, 2009, **131**, 124703.
- 104 Ç. Kılıç and A. Zunger, *Phys. Rev. Lett.*, 2002, **88**, 095501.



1182x570mm (72 x 72 DPI)

Using state-of-the-art hybrid DFT calculations we explain the defect chemistry of LaCuOSe, a poorly understood wide band gap p-type conductor.